land

MDPI

Article

Spatiotemporal Variation and Dynamic Simulation of Ecosystem Carbon Storage in the Loess Plateau Based on PLUS and InVEST Models

Kang Liu [1], Chaozheng Zhang [1], Han Zhang [1,*], Hao Xu [2] and Wen Xia [3]

[1] College of Economics and Management, Northwest A&F University, Xianyang 712100, China; kangliu@nwafu.edu.cn (K.L.); weirdo08@nwafu.edu.cn (C.Z.)
[2] School of Tourism and Resources and Environment, Ankang University, Ankang 725000, China
[3] School of Mathematics and Statistics, Ankang University, Ankang 725000, China
* Correspondence: hanzhang@nwafu.edu.cn; Tel./Fax: +86-18220826522

Abstract: Terrestrial ecosystems play an important role in carbon reduction and sequestration, and it is important to explore the carbon sequestration potential of terrestrial ecosystems under different land use scenarios to enhance the regional carbon storage potential. We analysed land use changes in the Loess Plateau, an important ecological barrier in China, from 2000 to 2020, used the PLUS model to predict land use patterns under different scenarios in 2035, and applied the InVEST model to assess carbon storage from 2000 to 2035. The findings were as follows: (1) Cropland in the study area decreased significantly from 2000 to 2020, and forests, waters, and construction land showed an increasing trend. The area of cropland further decreased under the natural growth and ecological protection scenarios, the area of grassland decreased significantly under the cropland protection scenario, and forests and waters were effectively protected under the natural development, ecological protection, and cropland protection scenarios. (2) Carbon storage in the Loess Plateau has increased by 28 Tg (0.56%) over the past 20 years. Compared with those in 2020, by 2035, carbon storage under the natural development, ecological protection, and cropland protection scenarios will increase by 30, 44, and 21 Tg, respectively. (3) Carbon storage has obvious spatial heterogeneity, with high carbon density in the northern Qinling Mountains, Taihang Mountains, and Lvliang Mountains and low carbon density in Erdos City and its surrounding areas. Regional differences in carbon density are closely related to the spatial distribution of land use types. (4) Carbon storage showed an inverted V-shaped trend with the increase in elevation. Land use change is the main reason for the increase or decrease in carbon storage under different scenarios. Compared with the other two scenarios, the ecological protection scenario not only protects the ecological environment but also has a strong carbon storage potential, which may be significant for guiding the formulation of future land use planning on the Loess Plateau.

Keywords: land use change; carbon storage; scenario simulation; PLUS model; InVEST model; the Loess Plateau

Citation: Liu, K.; Zhang, C.; Zhang, H.; Xu, H.; Xia, W. Spatiotemporal Variation and Dynamic Simulation of Ecosystem Carbon Storage in the Loess Plateau Based on PLUS and InVEST Models. *Land* **2023**, *12*, 1065. https://doi.org/10.3390/land12051065

Academic Editor: Stefan Gerber

Received: 12 April 2023
Revised: 7 May 2023
Accepted: 12 May 2023
Published: 13 May 2023

1. Introduction

Terrestrial ecosystems play an important role in carbon reduction and sequestration and are important links in the global carbon cycle [1]. Increased carbon storage in terrestrial ecosystems can effectively reduce greenhouse gases and is generally considered to be one of the most economically viable ways to reduce carbon sequestration [2,3]. As the most important manifestation of human activities, land use change leads to changes in carbon storage in terrestrial ecosystems [4,5]. Therefore, exploring the impact of land use change on terrestrial ecosystem carbon storage under the global 1.5 °C temperature control target and revealing the land use pattern and its carbon storage changes under different scenarios can help improve the carbon sequestration potential of terrestrial ecosystems from the

perspective of land use structure optimization, which is conducive to providing useful references for the decision-making of regional ecological environmental protection and carbon reduction and sequestration policies.

Land use scenario simulation plays a key role in quantifying the impact of land use change on ecosystem carbon storage [6]. In the early stages of research, scholars mostly used quantitative models, such as logistic regression [7], system dynamics [8], multi-objective planning [9], and ant colony optimization algorithms [10], to predict future land use demand. Because quantitative models cannot reveal the causal relationship between drivers and land use changes and cannot identify land use patterns spatially, coupled quantitative and spatial prediction models, such as Markov-CA [11], ANN-CA [12], Logistic-CA [13], and CLUE-S [14,15], have gradually become new research tools. However, in the actual prediction process, the CA model does not set a mechanism to restrict the metacell state transformation and cannot simulate multiple land use types [16]; the CLUE-S model ignores the probability problem of disadvantaged land use types in the allocation process [17], which leads to large prediction errors and is mostly applied to small-scale studies [18]. Although the FLUS model can solve the above problems better and has a higher prediction accuracy than the CLUE-S and CA models [19], it is difficult to simulate the spatial and temporal dynamics of multiple land use types at the patch level [20]. To solve this problem, the PLUS model applies a new land expansion analysis strategy (LEAS) to better explore the causal factors of land use change while being able to accurately simulate patch-level changes in multiple types of land use and has achieved good results in prediction studies [21–23].

Compared to the field survey method [24], the InVEST model has achieved good results in the dynamic assessment and scenario simulation of carbon storage in the context of land use change because of its simplicity and reliability, low data demand, fast operation speed, and suitability for multiscale studies [25–27]. In addition, further quantification of the effects of elevation and different land use scenarios on ecosystem carbon storage can help guide the formulation of policies for coordinated ecological protection and economic development more precisely. Previous studies have shown that the carbon storage of the Qinba Mountains shows a trend of increasing and then decreasing with increasing elevation [21,28]. Zhu et al. [29] found that the trend of carbon density in the Qi River basin showed an "N" shape with increasing altitude and made targeted suggestions for coordinating cropland protection and increasing carbon storage potential.

The Loess Plateau is the core area of the ecological protection and high-quality development strategy of the Yellow River Basin as well as an important ecological barrier and key area for ecological construction in China. In recent years, continuous human activities and major ecological projects, such as the return of cropland to forest (grass), have led to dramatic changes in land use and land cover [30,31]; thus, the study of ecosystem carbon storage has attracted academic attention. Most studies have assessed the status of ecosystem carbon storage using field surveys and single-ecosystem carbon storage has been the focus of attention. Researchers have measured the carbon storage of grasslands [32–34], forests [35,36], and a single carbon pool, such as the soil on the Loess Plateau [37]. In addition, previous studies have explored the effects of environmental variables such as climate, topography, soil, and vegetation cover on ecosystem carbon storage and spatial patterns [31,38,39].

The above results provide scientific knowledge for the study of carbon storage in the Loess Plateau ecosystem. However, there are still several shortcomings. First, the field survey method is not suitable for large-scale and long-term time series studies and cannot capture the spatial and temporal patterns and evolution of carbon storage dynamically. Moreover, the study of a single ecosystem or carbon pool cannot comprehensively reflect the status and development trend of carbon storage in terrestrial ecosystems. Second, existing studies did not pay sufficient attention to the simulation of future land use scenarios and the resulting changes in carbon storage, thus making it difficult to provide effective support for the optimization of land use structure and decision-making under low-carbon development

goals. Third, the carbon density of existing studies was mostly based on carbon intensity data from geographically similar regions [6,25,26], which may have led to a deviation in the carbon density data from the actual study area and made the final measured ecosystem carbon storage inaccurate.

Considering this, this study analyzed land use changes on the Loess Plateau from 2000 to 2020 and used the PLUS model to predict land use patterns under different scenarios in 2035. Spatial and temporal changes in the ecosystem carbon storage on the Loess Plateau from 2000 to 2035 were assessed using the InVEST model by integrating field measurement data from the Chinese terrestrial ecosystem carbon density dataset on the Loess Plateau and carbon density correction data. This study aimed to offer insights into the following questions: (1) How has the land use pattern of the Loess Plateau changed after the implementation of a major ecological project of returning cropland to forest (grass) for more than 20 years? What are the trends in the spatial and temporal patterns of ecosystem carbon storage due to land use change? (2) How will the future land use patterns of the Loess Plateau change under different development scenarios? (3) What is the potential for carbon sequestration under different development scenarios? (4) Which development scenarios are suitable for the realistic needs of the study area? Timely answers to these questions can provide beneficial references for the preparation of territorial spatial planning and carbon reduction and sequestration strategies in the Loess Plateau, which can also provide scientific suggestions for ecological environmental protection and carbon storage potential enhancement in the study area.

2. Materials and Methods

2.1. Study Area

The Loess Plateau is located between 33°41′ and 41°16′ N and 100°52′ and 114°33′ E, spanning seven provinces in Shanxi, Henan, Shaanxi, Inner Mongolia, Ningxia, Gansu, and Qinghai, with an area of about 635,000 km^2. The Loess Plateau is characterized by a large undulating terrain and ravines, making it one of the regions with the most severe soil, water loss, and soil erosion worldwide. At the same time, it is also a highly fragile ecological environment [38]. After more than 20 years of reforestation and ecological projects, the land cover of the Loess Plateau has significantly improved [30,31]. Therefore, using the Loess Plateau as a typical case study to dynamically simulate carbon sequestration potential under different land use scenarios is of great practical significance for enhancing the carbon storage potential of the ecosystem in the study area and improving the regional ecological environment (Figure 1).

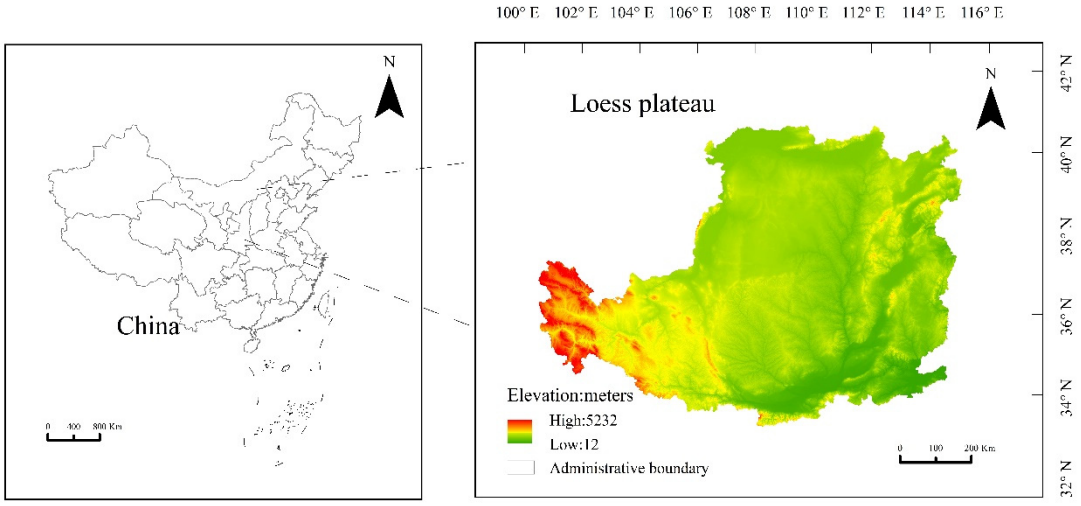

Figure 1. Location and administrative division map of the study area.

2.2. Data Sources and Processing

2.2.1. Date Sources

The data used in this study included land use data, administrative boundary data, and land use change driver data from the Resource and Environment Science and Data Center of the Chinese Academy of Sciences (http://www.resdc.cn, accessed on 1 April 2023.). After cropping and projection, the land use data were reclassified into six categories: cropland, forest, grassland, water, construction land, and unused land. Considering the characteristics of severe soil and water loss and soil erosion in the study area, data on soil type, soil erosion, and soil texture (silty soil content, clay content, and sand content) were added to simulate land -use changes more accurately. The final 17 selected drivers included natural factors, such as topography, climate, soil, and water systems, as well as socioeconomic factors, such as population, economic development level, and traffic accessibility (Table 1).

Table 1. Date sources.

Data Category	Data Subcategory	Data Name	Rormat	Unit/Interval
Land use	Land use maps in 2000, 2005, 2010, 2015, and 2020		Raster	6 type variables
Administrative boundary	Administrative boundary of the Loess Plateau		Vector	None
Natural factors	Topography	Elevation	Raster	m
		Slope	Raster	°/[0, 90]
	Climate	Average annual precipitation	Raster	mm
		Average annual temperature	Raster	°C
	Soil	Soil type	Raster	15 type variables
		soil erosion	Raster	3 type variables
		Silty soil content	Raster	%/[0, 100]
		Clay content	Raster	%/[0, 100]
		Sand content	Raster	%/[0, 100]
	River system	Distance to river	Vector	km
Socioeconomic factors	Population	Population density	Raster	Person/km^2
	Economic development level	GDP	Raster	10,000 yuan/km^2
	Traffic accessibility	Distance to urban first-class road	Vector	km
		Distance to railway	Vector	km
		Distance to national highway	Vector	km
		Distance to provincial highway	Vector	km
		Distance to highway	Vector	km

2.2.2. Processing of Land Use Change Driver Data

The scenario simulation of future land use patterns using the PLUS model requires the processing of land use change driver data to satisfy the software's operational requirements. Using ArcGIS 10.8, the elevation, temperature, precipitation, silty soil content, clay content, and sand content were visualized. Soil types consisted of 227 subclasses, which were classified into 11 soil classes using the "reclassification" tool in ArcGIS 10.8, and soil erosion was classified into three classes: wind erosion, hydraulic erosion, and freeze–thaw erosion, using the same method. The slope was extracted from elevation with the help of ArcGIS, and the river and road distances were obtained by performing buffer analysis using the "Euclidean distance" tool. All data were analyzed using ArcGIS software to unify the administrative boundaries based on the Loess Plateau, and the data resolution size was adjusted to 100 m × 100 m using a raster resampling tool (Figure 2).

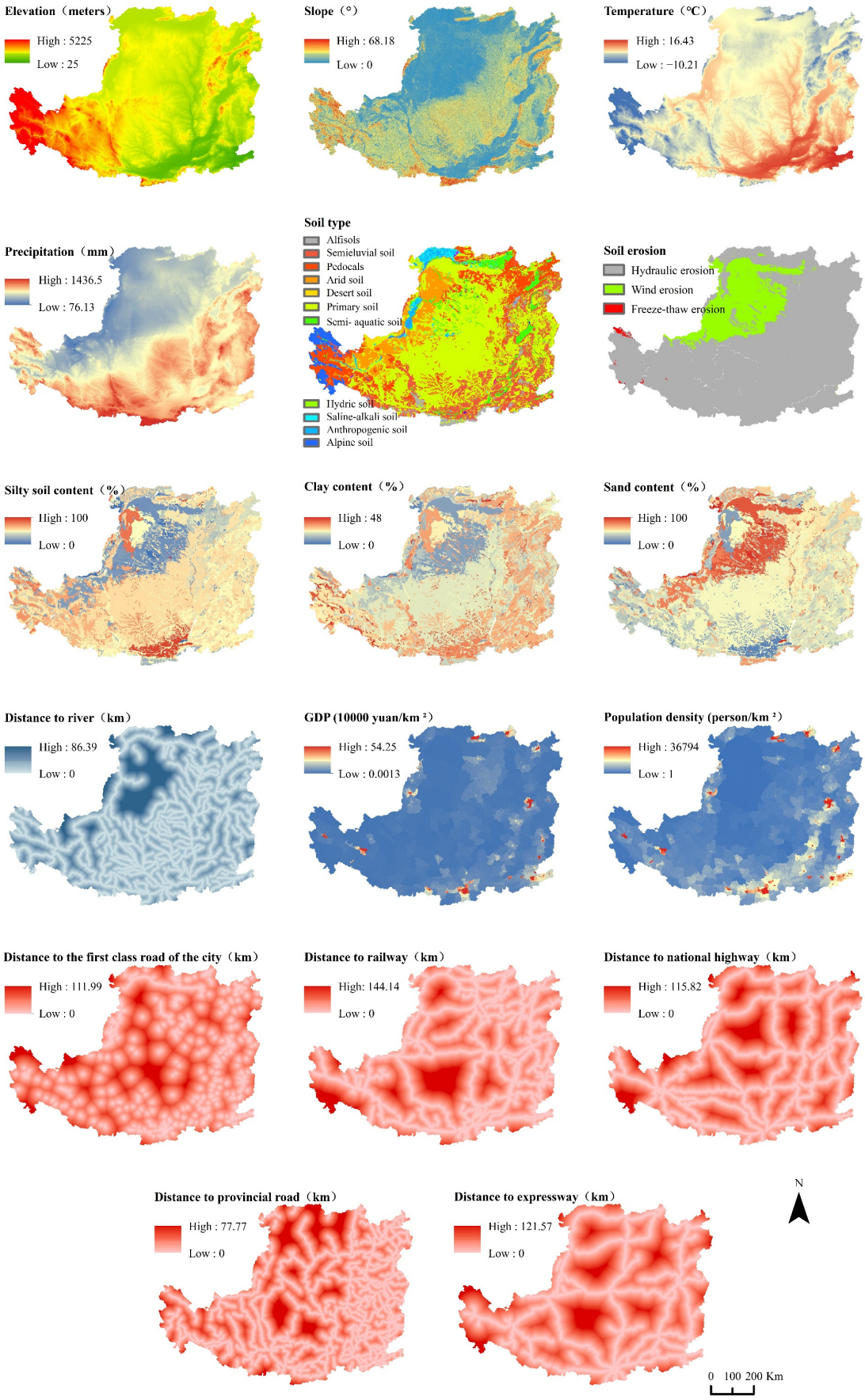

Figure 2. Land use change drivers.

2.3. Research Methodology

2.3.1. Prediction of Land Use Change Based on the PLUS Model

The PLUS model is a policy-driven land use scenario simulation and prediction model that can be developed based on the FLUS model. The model is mainly used to simulate fine-scale land use changes and provides a basis for policymakers to evaluate, plan, and manage land, ecological, and landscape systems for decision-making [40]. Parameters and processes of the PLUS model were set as follows:

(1) Watershed was set as a restricted transformation area. (2) Land expansion analysis strategy (LEAS). On 10 January 2002, the Western Development Office of the State Council decided to fully launch the project of returning farmland to forests, which had a certain impact on land use and land cover. Therefore, in this study, we input land use data from 2005 and 2010 into the LEAS module, extracted the areas with changes in each land use type, randomly extracted the sampling points for analysis, and then used the random forest algorithm to mine the land use change rules through the training dataset to predict the land use pattern in 2020. After accuracy verification, we input land use data from 2005 and 2020 into the LEAS module, used the same algorithm to obtain the development probability of each land use type, and then predicted the land use pattern under different scenarios in 2035. (3) A CA model based on multiclass random patch seeds (CARS) which combined random seed generation and threshold-decreasing mechanisms was used to simulate the automatic generation of patches under the constraints of development probability. (4) Based on land use data from 2005 and 2010, future land demand was predicted using the historical land transfer probability matrix with the help of the Markov module. (5) Setting neighborhood weights. According to the proportion of land use expansion area and transfer probability, combined with the accuracy of land use simulation in 2020 and the kappa coefficient, the simulation results were optimized through several rounds of debugging, and the transfer elasticity of each land use type was finally determined (Table 2). (6) Model accuracy verification. The PLUS model was validated using overall accuracy (OA) and kappa coefficient to ensure the applicability of the model in the study area. Both the OA and kappa coefficients were in the range of 0–1. The higher the value of 1, the higher the simulation accuracy. When the value exceeds 0.75, the accuracy of the simulation is reliable [20,40]. The accuracy verification of the current land use situation in 2020 and the prediction results in 2020 showed that the OA was 87.55% and the kappa coefficient was 0.8224 in this paper, indicating that the simulation was highly accurate and could satisfy the research requirements.

Table 2. LEAS values of land use types under different scenarios.

Scenario	Cropland	Forest	Grassland	Waters	Construction Land	Unused Land
2000–2020/Q1	0.42	0.15	0.03	0.01	0.34	0.05
Q2	0.42	0.16	0.04	0.01	0.34	0.03
Q3	0.45	0.15	0.03	0.01	0.32	0.04

By combining the development status and actual needs of the study area and drawing on the relevant studies [6,29], this study sets up three land use scenarios with different needs. (1) Under the natural growth scenario (Q1), the conversion order of each land use type is construction land, forest, cropland, waters, grassland, and unused land. (2) Under the ecological protection scenario (Q2), ecological land, such as forests, grasslands, and water, must be strictly protected, and the conversion order of the various types of land is forest, grassland, cropland, water, construction land, and unused land. (3) Under the cropland protection scenario (Q3), the rate of encroachment of construction land into other land, especially cropland, must be curbed and the rate of transfer of cropland to other land types must be reduced. Under Q3, all land other than construction land can be converted into cropland. Based on the principle of not allowing the conversion of high-grade land to

low-grade land, a cost conversion matrix was established, and the LEAS values of land use types were developed by combining land use demands under different scenarios (Table 2).

2.3.2. Ecosystem Carbon Storage Assessment Based on the InVEST Model

Carbon storage was calculated based on the InVEST model, which simulates carbon storage based on the land use data of each period and the corresponding carbon density using the following formula:

$$C_{tot} = \sum_{i=1}^{n} (C_{i\_above} + C_{i\_below} + C_{i\_soil} + C_{i\_dead}) \times A_i. \quad (1)$$

In Equation (1), C_{tot} denotes the total ecosystem carbon storage; C_{i_above}, C_{i_below}, C_{i_soil}, and C_{i_dead} denote the aboveground carbon density, belowground carbon density, soil carbon density, and dead organic carbon density of the i-th type of land use, respectively; A_i is the area of land use type i; n is the number of land use types; nd n in this study is 6.

Drawing on the relevant studies in the Loess Plateau area [6,25], as shown in Table 3, the dead organic carbon density for each land use type was obtained. The soil carbon density data for cropland, grassland, and forest were obtained from the Chinese Terrestrial Ecosystem Carbon Density Dataset [41]. The data acquisition process was as follows: first, the latitude and longitude coordinates of the soil carbon density collection points at 20 cm and 100 cm belowground in China were imported into ArcGIS 10.8. Second, the soil carbon density collection points distributed in the study area were obtained by cropping with the administrative boundary of the Loess Plateau, and 215, 169, and 179 collection points at 20 cm belowground (Figure 3a), and 213, 165, and 169 collection points at 100 cm belowground (Figure 3b) of cropland, grassland, and forest land were obtained. Finally, the average values of the collection points at 20 cm and 100 cm belowground were used as the soil carbon density of cropland, grassland, and forest land (Table 3).

Table 3. Carbon density of different land use types (t/hm^2).

Land Use Type	$C_{\_below}$	$C_{\_below}$	$C_{\_soil}$	$C_{\_dead}$
Cropland	5.58	1.06	41.82	13
Forest	69.06	18.30	49.05	13
Grassland	3.33	20.45	48.49	2
Waters	0.06	0	52.53	0
Construction land	0.36	0	58.36	0
Unused land	0.06	0	53.68	0

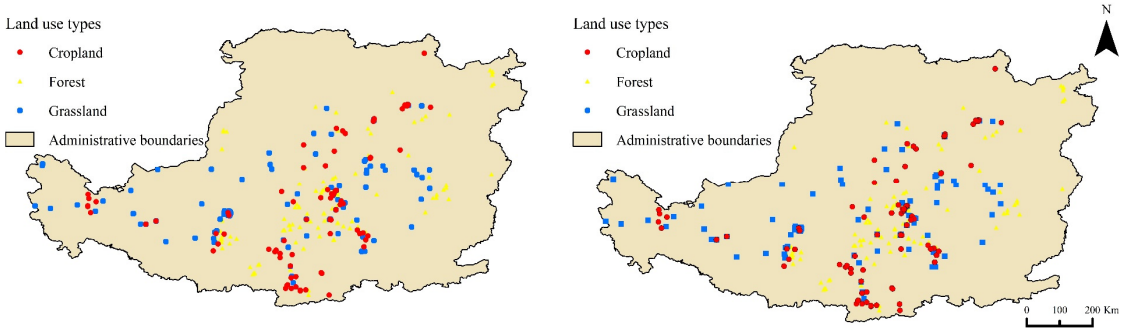

a. Soil carbon density collection points at 20 cm below ground b. Soil carbon density collection points at 100 cm below ground

Figure 3. Distribution of soil carbon density collection points.

The aboveground and belowground biomass carbon density data of cropland, grassland, and forest at the national level were obtained based on a relevant study by Li et al. [42] and were combined with the root-to-stem ratio of crops [43–45]. The aboveground biomass

carbon density and soil carbon density data for construction land, water, and unused land in Jiangsu Province were obtained by referring to Tui et al. [46], and the belowground biomass carbon density data were obtained by referring to Zhu et al. [29]. Finally, the data were modified to the actual carbon density data of the Loess Plateau (Table 3) by referring to the relationship models of soil carbon density and biomass carbon density with temperature and precipitation by Chen et al. [47] and Alam et al. [48].

$$C_{BP} = 6.798 \times e^{0.0054 \times MAP} \quad (2)$$

$$C_{BT} = 28 \times MAT + 398 \quad (3)$$

$$C_{SP} = 3.3968 \times MAP + 3996.1 \quad (4)$$

$$K_{BP} = C_{BP}^{1} / C_{BP}^{2} \quad (5)$$

$$K_{BT} = C_{BT}^{1} / C_{BT}^{2} \quad (6)$$

$$K_{B} = K_{BP} \times K_{BT} \quad (7)$$

$$K_{SP} = C_{SP}^{1} / C_{SP}^{2} \quad (8)$$

In Equations (2)–(8), *MAP* represents the average annual precipitation, which is 628 mm, 1040.4 mm [28,29], and 418.73 mm [49] for the whole country, Jiangsu Province, and the Loess Plateau, respectively; *MAT* represents the average annual temperature, which is 9 °C, 15.7 °C [28,29], and 11.21 °C [50] for the whole country, Jiangsu Province, and the Loess Plateau, respectively. *CBP* and *CSP* denote the biomass carbon density and soil carbon density, respectively, obtained after correction according to precipitation; *CBT* denotes the biomass carbon density obtained after correction according to the average annual temperature; *KBP* and *KBT* denote the correction coefficients of the annual average precipitation factor and the annual average temperature factor for aboveground biomass carbon density, respectively; *KB* and *KSP* denote the correction coefficients of aboveground biomass carbon density and soil carbon density, respectively; C^1 and C^2 are the corresponding data obtained from the study area and the whole country and the study area and Jiangsu Province based on the average annual precipitation and average annual temperature, respectively.

3. Results

3.1. Land Use Change Characteristics and Scenario Analysis of the Loess Plateau

3.1.1. Analysis of Land Use Change from 2000 to 2020

Analysis of the magnitude of land use change (Figure 4a,b) revealed that the land use type of the Loess Plateau is dominated by grassland and cropland, accounting for more than 30% of the area, followed by forest, unused land, construction land, and waters. The proportion of cropland area decreased from 33.03% in 2000 to 30.97% in 2020, representing a decrease of 2.06%. The grassland and unused land areas showed small downward trends, from 41.55% and 6.88% in 2000 to 41.44% and 6.61% in 2020, respectively, with a decline of less than 0.3%. The areas of construction land, forest, and water showed different degrees of expansion, increasing from 2.40%, 14.76%, and 1.38% in 2000 to 4.23%, 15.33%, and 1.42% in 2020, respectively, with the largest increase of 1.83% for construction land. In terms of spatial distribution, cropland is mainly concentrated in the Hetao, Datong, XinDing, Taiyuan, Changzhi, Yuncheng, and Guanzhong plains, which are flat, have fertile soil, and are mostly distributed along both sides of rivers, such as the Yellow, Jing, Wei, and Fen Rivers. Forests are mainly distributed at the northern foot of the Qinling Mountains, on

both sides of the Taihang Mountains, and in Lvliang Mountains. After the implementation of the ecological project of returning cropland to forest, there is an obvious trend of forest expansion in some areas of Yan'an, Yulin, and Ordos cities. Construction land is mosaically distributed within the cropland and shows a trend of expansion along the Guanzhong Plain and Fen River in all directions. Unused land is mainly concentrated in Ordos.

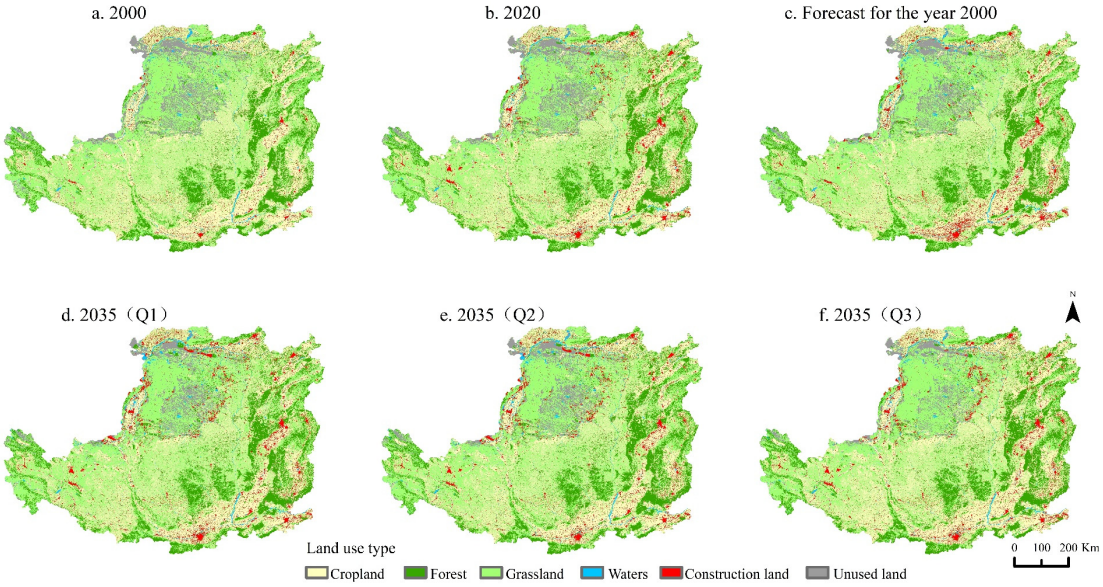

Figure 4. Current situation and prediction of land use in the study area.

Analysis of land use type transfer (Table 4) revealed that more than 50% of the cropland was transferred to grassland, 40.21% was transferred to forest and construction land, and the remaining small portion was transferred to waters and unused land, which was closely related to the ecological project of returning cropland to forest (grass). Of the total cropland area, the area transferred out was 1.68 times that of the area transferred in, reducing the total cropland area on the Loess Plateau by 12,882.45 km^2 over the past 20 years, which indicates that the Loess Plateau must reduce the encroachment on cropland in future socioeconomic development and industrial construction and abide by the three red lines of cropland protection to ensure cultivated land and food security. More than 50% of the forest was transferred to grassland, and the area transferred in was 1.5 times that of the area transferred out, mostly from grassland and cropland. Grassland transferred out more than 50% area to cropland, and the transferred-in area was slightly larger than that transferred out; most of the transferred-in land types were cropland and forest land. More than 75% of the construction land was transferred to croplands, and the transferred-in area was six times that of the transferred-out area, which was mostly from croplands and grasslands. The transferred-out and transferred-in areas of water were essentially equal. The transferred-out area of unused land was 1.37 times that of the transferred-in area. More than 60% of the unused land was transferred to grasslands.

Table 4. Land use transfer matrix of the Loess Plateau from 2000 to 2020 (km^2).

2000	2020							
	Cropland	Forest	Grassland	Waters	Construction Land	Unused Land	Total	Transferred Out
Cropland	175,235.86	4179.87	17,347.77	1038.82	8614.82	640.57	207,057.71	31,821.85
Forest	2043.6	85,495.14	3990.78	154.04	691.41	176.59	92,551.56	7056.42
Grassland	13,549.37	5756.39	233,766.97	682.41	3494.72	3284	260,533.86	26,766.89
Waters	730.29	119.21	550.8	6623.85	254.03	357.63	8635.81	2011.96
Construction land	1760.72	105.68	333.41	57.41	12,754.49	32.89	15,044.6	2290.11
Unused land	855.42	432.05	3824.17	344.16	709.51	36,944.75	43,110.06	6165.31
Total	194,175.26	96,088.34	259,813.9	8900.69	26,518.98	41,436.43	626,933.6	—
Transferred in	18,939.4	10,593.2	26,046.93	2276.84	13,764.49	4491.68	—	76,112.54

3.1.2. Analysis of Land Use Change Scenarios

Figure 4d–f shows the projected land use results of the study area under different scenarios, and Table 5 shows the changes in land use area of each land use type under different scenarios compared to 2020. In general, both the natural growth and ecological protection scenarios show that the area of cropland and unused land decreases, and the area of forest, grassland, waters, and construction land increases. Under the cropland protection scenario, the area of grassland and unused land decreases while that of cropland, forest, water, and construction land increases.

Table 5. Comparison of area of different categories in 2035 and 2020 under different scenarios.

Land Use Type	2020	2035			Changes in 2020–2035		
		Q1	Q2	Q3	Q1	Q2	Q3
	Area/km^2 Proportion/%	Area/km^2 Proportion/%	Area/km^2 Proportion/%	Area/km^2 Proportion/%	Area/km^2 Proportion/%	Area/km^2 Proportion/%	Area/km^2 Proportion/%
Cropland	194,175.26 (30.97)	190,544.72 (30.39)	190,544.72 (30.39)	219,475.05 (35.01)	−3630.54 (−1.87)	−3630.54 (−1.87)	25,299.79 (13.03)
Forest	96,088.34 (15.33)	98,487.78 (15.71)	100,103.09 (15.97)	100,103.09 (15.97)	2399.44 (2.50)	4014.75 (4.18)	4014.75 (4.18)
Grassland	259,813.9 (41.44)	263,355.66 (42.00)	263,355.66 (42.01)	241,263.6 (38.48)	3541.76 (1.36)	3541.76 (1.36)	−18,550.3 (−7.14)
Waters	8900.69 (1.42)	10,397.32 (1.66)	10,415.25 (1.66)	9056.88 (1.44)	1496.63 (16.81)	1514.56 (17.02)	156.19 (1.75)
Construction land	26,518.98 (4.23)	32,195.29 (5.14)	28,721.13 (4.58)	29,581.35 (4.72)	5676.31 (21.40)	2202.15 (8.30)	3062.37 (11.55)
Unused land	41,436.43 (6.61)	31,952.83 (5.10)	33,793.75 (5.39)	27,453.63 (4.38)	−9483.6 (−22.89)	−7642.68 (−18.44)	−13,982.8 (−33.75)

Viewed by land type, the cropland area decreases by 3630.54 km^2 under Q1 and Q2, with a decrease of 1.87%, and increases by 25,299.79 km^2 under Q3, with an increase of 1.87%. Forests are effectively protected under all three scenarios, and the increase in forest area under Q2 and Q3 (4.18%) is greater than that under Q1 (2.50%). Compared to 2020, the forest continues to expand in all directions along the northern Qinling Mountains and on both sides of the Taihang and Lvliang Mountains. The grassland area increases by 3541.76 km^2 under Q1 and Q2, with an increase of 1.36%, while it decreases by 18,550.3 km^2 under Q3, which is a greater decrease compared to Q1 and Q2. Most of the grassland area is replaced by cropland under Q3. Water increases in all three scenarios, with the largest increase (17.02%) in Q2 and a smaller increase (1.75%) in Q3, with an evident expansion of water around the Hetao Plain, Erdos City, and Fen River. Construction land expands in all three scenarios, showing a circular expansion centered on settlements and an axial expansion along both sides of the rivers and roads. The expansion of construction land under Q1 reaches 5676.31 km^2, with an expansion rate of more than 20%; the expansion rate under Q3 reaches 11.55%; and the expansion rate under Q2 is smaller (8.30%). The

unused land area reduces by 9483.6 km^2, 764.2 km^2, and 13,982.8 km^2 under Q1, Q2, and Q3, respectively; a large amount of unused land is transferred to cropland under Q3.

3.2. Temporal Change Characteristics of Carbon Storage in the Loess Plateau Ecosystem

3.2.1. Analysis of Carbon Storage Measurement Results from 2000 to 2020

As shown in Figure 5a, the carbon storage and carbon density of the ecosystem in the study area have been increasing annually over the past 20 years, from 4.956 Pg and 79.05 t/hm^2 in 2000 to 4.984 Pg and 79.50 t/hm^2 in 2020, respectively. Thus, the net carbon storage increased by 28 Tg, with an increase of 0.56% and an average annual increase of 1.4 Tg. The increase in carbon density was 0.45 t/hm^2 and showed an increase of 0.57%. This indicates that the national ecological project of returning cropland to forest and grass in the study area not only improved land cover, but also played a positive role in increasing the carbon sink and improving the ecological environment.

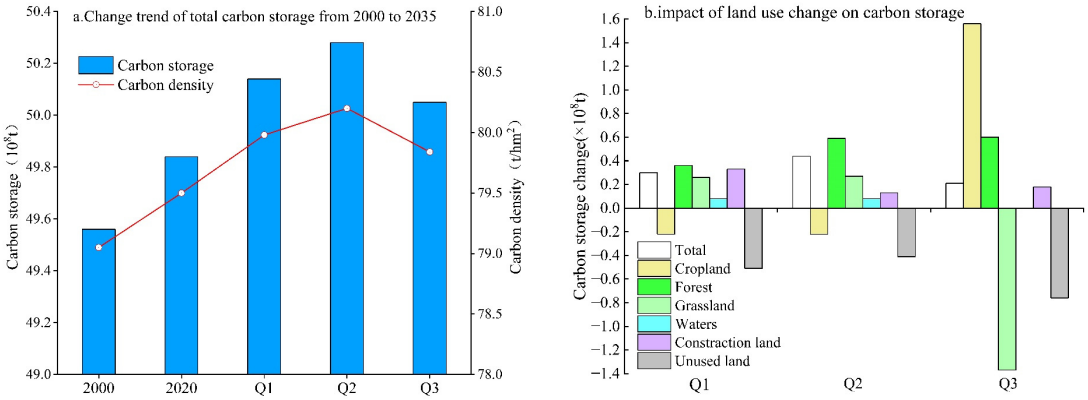

Figure 5. Change trend of total carbon reserves and local carbon reserves from 2000 to 2035.

Based on land type, in the past 20 years, the total amount of carbon storage in grassland was the largest, followed by that in forest and cropland, and the sum of the three accounted for more than 90% of the total carbon storage. The percentage of carbon storage in water, construction land, and unused land was less, and the sum of the three accounted for less than 10%. The total amount and proportion of carbon storage in cropland showed a decreasing trend, with a decrease of 80 Tg over the past 20 years, an increase of 6.28%, and an average annual decrease of 4 Tg. The total amount and proportion of carbon storage in forest land showed an increasing trend, with an increase of 53 Tg over 20 years, an increase of 3.83%, and an average annual increase of 2.65 Tg. The total amount and proportion of carbon storage in grassland and water were relatively stable, whereas that in construction land increased from 88 to 156 Tg, and that in unused land decreased from 232 to 223 Tg (Figure 5b).

3.2.2. Analysis of Carbon Storage Projection Results under Different Scenarios

Overall, compared with 2020, carbon storage and carbon intensity in 2035 show an increasing trend in all three scenarios (Figure 5a). Under Q1, the carbon storage and carbon density will reach 5.014 Pg and 79.98 t/hm^2, an increase of 30 Tg and 0.48 t/hm^2, respectively, and under Q2, they will reach 5.028 Pg and 80.2 t/hm^2, an increase of 44 Tg and 0.7 t/hm^2, respectively. Under Q3, the carbon storage and carbon density will reach 5.005 Pg and 79.84 t/hm^2, an increase of 21 Tg and 0.34 t/hm^2, respectively. Therefore, the cropland protection scenario has the slowest growth rate of carbon storage, whereas the ecological protection scenario can effectively increase carbon storage and has the highest carbon sequestration potential.

Based on land type, the carbon storage of grassland in all three scenarios exceeded 35%, that of forest was approximately 30%, the sum of the carbon storage of construction land, unused land, and water was less than 10%, and the carbon storage of cropland in Q3

(26.95%) was higher than that of the other two scenarios (approximately 23%). Compared to 2020, the carbon storage of forest, grassland, water, and construction land under Q1 and Q2 will increase to different degrees, whereas the carbon storage of cropland and unused land will decrease. Under Q3, the carbon storage of grassland and unused land significantly decreased by 137 Tg and 76 Tg, respectively, whereas other land types showed an increase (Figure 5b).

3.3. Spatial Change Characteristics of Carbon Storage in the Loess Plateau Ecosystem

3.3.1. Spatial Distribution Pattern of Carbon Storage

Figure 6 shows that the carbon storage of the Loess Plateau ecosystem has obvious spatial heterogeneity, with the highest value of 149.41 t/hm^2 and the lowest value of 52.59 t/hm^2. The Jenks method was used to classify the carbon density of the study area into low-, medium-low-, medium-high-, and high-value areas, with interruption points of 53.74 t/hm^2, 61.46 t/hm^2, and 74.27 t/hm^2, respectively. As shown in Figure 6a,b,d–f, the areas with high carbon storage values are concentrated in the southeastern part of the study area in the form of strips, and the highest carbon density is distributed in the northern Qinling Mountains, Taihang Mountains, and Lvliang Mountains, which are mainly forests with high vegetation cover and thus have strong carbon storage potential. The low-value areas of carbon storage are concentrated in the north-central region of the study area in the form of clusters, and the land use types in these areas are mainly unused land and water. The medium-high and medium-low areas of carbon storage are staggered, and most of the land types are cropland, grassland, and construction land, which are the main land use types in the study area; the areas of medium-high and medium-low carbon storage account for more than 75% of the total study area. In addition, the spatial distribution patterns of carbon storage in the three future scenarios were similar to those in 2020.

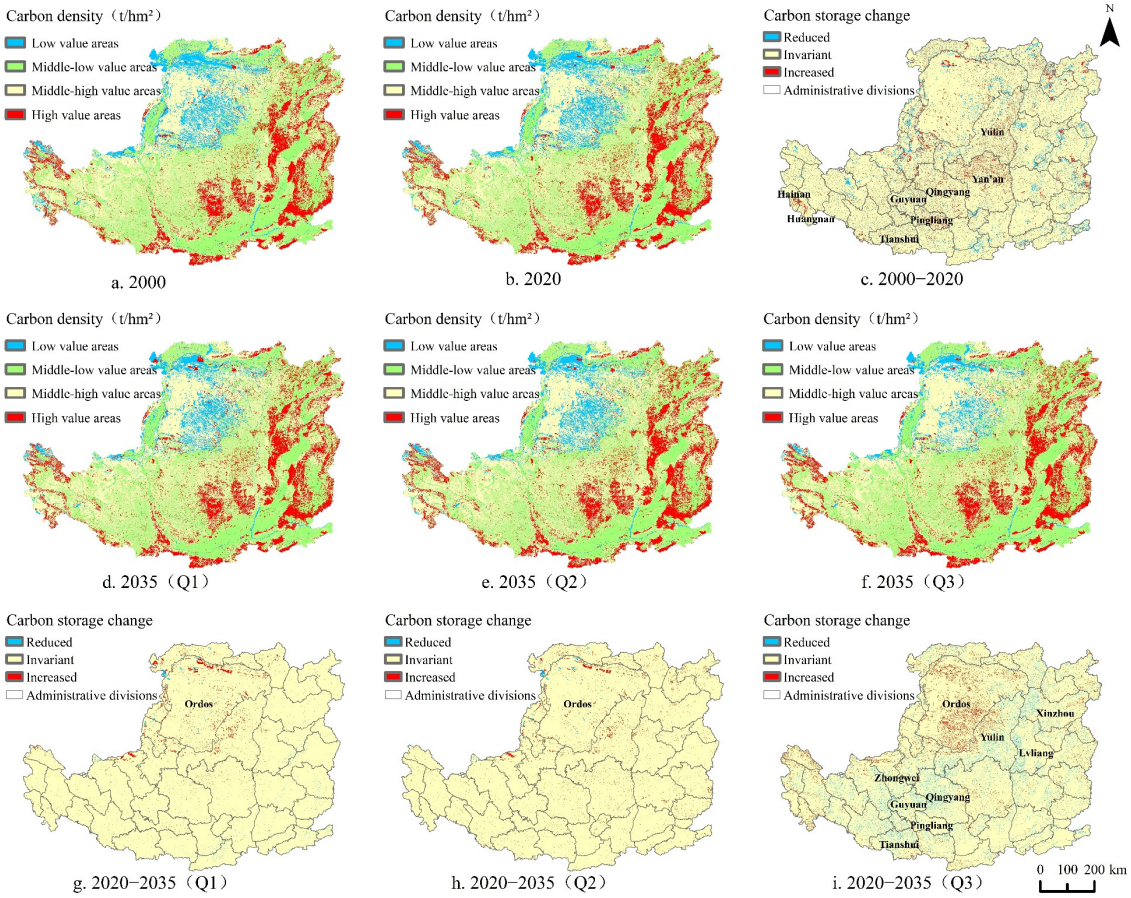

Figure 6. Spatial pattern and change of carbon storage in the study area from 2000 to 2035.

3.3.2. Increase and Decrease in the Spatial Distribution of Carbon Storage

Spatial changes in carbon storage were divided into three categories: reduced, increased, and invariant. As shown in Figure 6c,g–i, the change in carbon storage was mainly invariant, but the spatial change in carbon storage in 2020 and the different scenarios showed some variability.

From 2000 to 2020, the areas of the decreased and increased regions were 38,795.59 km^2 and 37,316.95 km^2, respectively, while 87.86% maintained carbon storage. The carbon storage loss was significant in central Lanzhou, northern Xi'an, northwestern Tongchuan, northwestern Lvliang, southeastern Taiyuan, central Yangquan, central Linfen, northwestern Zhengzhou, and northeastern Luoyang. Owing to urban expansion and other human activities, a large amount of cropland and forest in the abovementioned regions has been converted into construction land, decreasing regional carbon storage and carbon density. The increased carbon storage occurred in several areas in the study area and was obvious in Yulin, Yan'an, Qingyang, Pingliang, Guyuan, Tianshui, the southern part of Hainan State, and the northwestern part of Huangnan State. The main reason for the increase in carbon storage was the conversion of cropland and unused land into forests and grasslands. In addition, a series of projects, such as inner-city greening, watershed and wetland improvement, and ecological management of urban–rural combinations, also played an active role in improving the ecological environment and enhancing carbon storage services.

From 2020 to 2035, the percentages of the increased regions in carbon storage were 1.59% and 1.99% under Q1 and Q2, respectively, and the percentages of the decreased regions in carbon storage were 0.5% and 0.24% under Q1 and Q2, respectively, while the remaining areas remained invariant. The increase in carbon storage within Ordos and the border regions was evident, mainly because of the conversion of a large amount of unused land into grassland and forest land. Under Q3, the percentage of the increased regions in carbon storage was approximately 3.34%, which was influenced by the conversion of unused land into grassland and woodland; the increase in carbon storage in Erdos and northwest Yulin was obvious. The decrease in carbon storage in southeastern Yulin, Xinzhou, Lvliang, Qingyang, Pingliang, Zhongwei, Guyuan, and Tianshui was approximately 4.30% and was associated with a significant reduction in the area of grassland and unused land due to strict cropland protection. In summary, the spatial distribution pattern of carbon storage and changes in spatial distribution (increased and decreased) were found to be closely related to the spatial distribution of land use types in the study area.

4. Discussion

4.1. Effect of Elevation on Ecosystem Carbon Storage

The effect of elevation on ecosystem carbon storage was investigated by reclassifying the elevation into 11 categories using a reclassification tool, with every 500 m acting as an interruption point. As shown in Figure 7a, the carbon storage in the study area changed with elevation, showing an inverted "V" shape trend of increasing and then decreasing. Ecosystem carbon storage showed a slow increase from 500 to 1000 m, a sharp increase from 1000 to 1500 m, and a peak at 1500 m. After the peak, the ecosystem carbon storage decreased rapidly at 1500–2500 m. Above 2500 m, the ecosystem carbon storage decreased slowly. Overall, the carbon storage potential was the highest in the elevation range of 1000–2000 m, with 66% of the ecosystem carbon storage in the study area; the elevation ranges of 500–1000 m and 2000–2500 m show the second highest storage potential, and storage potential in other elevation ranges was low. The carbon storage in the Qinba Mountains, located in the southern part of the study area and have similar longitudes (101°–114° E) to the Loess Plateau, also shows the same inverted "V" shape trend with increasing altitude, and the carbon storage is most abundant in the 800–2000 m area [21,28], which is largely consistent with the findings of our research.

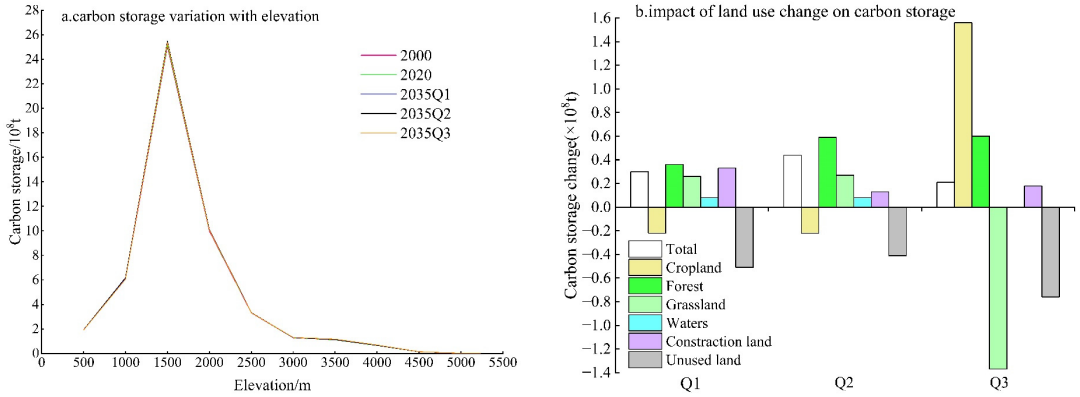

Figure 7. Impact of elevation and land use change on ecosystem carbon storage.

4.2. Effects of Land Use Change on Ecosystem Carbon Storage

Compared to 2020, the ecological protection scenario had the highest carbon sequestration potential, followed by the natural growth scenario, while the cropland protection scenario had the lowest growth rate of total carbon storage. The changes in carbon storage of each land use type in different scenarios (Figure 7b) indicate that land use change is the main reason for the differences in ecosystem carbon storage under different scenarios.

Under Q1, cropland and unused land decreased by 3630.54 km^2 and 9483.6 km^2, respectively. Therefore, the carbon storage of cropland and unused land decreased by 22 Tg and 51 Tg, respectively, which is an important reason for the slow increase in carbon storage under this scenario. Under Q2, the expansion of construction land was effectively curbed (the expansion rate is the smallest), and the expansion rates of forest land, grassland, and water area were the highest in all three scenarios, which indicates that this scenario is important for protecting the ecological environment and increasing the carbon storage potential in the study area. Therefore, the ecological protection scenario is consistent with the strategic positioning of ecological barriers and is worthy of further promotion. Under Q3, although the amount of cultivated land was guaranteed, the areas of grassland and unused land simultaneously decreased significantly. Therefore, the carbon storage of grassland and unused land in this scenario decreased by 137 and 76 Tg, respectively, which led to the lowest growth rate of total carbon storage in this scenario.

Previous studies have predicted carbon storage in the Qi River Basin [29] and the Fen River Basin [51] (both located in the Loess Plateau region). The results show that carbon storage and carbon density will increase significantly under the ecological protection scenario compared with the natural growth scenario, and the ecological conservation scenario will not only enhance the carbon sequestration potential but also effectively protect the ecological environment in the study area. These findings indicated that the scenario simulation results of our study are reliable to a certain extent.

4.3. Policy Implications

The rapid expansion of construction land and a significant reduction in cropland under the natural growth scenario are not conducive to the sustainable development of the study area. The ecological protection scenario can effectively curb the expansion rate of construction land and help further improve the fragile ecological environment in the study area while protecting forests, grasslands, and water; this scenario has the highest carbon sequestration potential. The cropland protection scenario can increase the area of cropland but squeeze out a large amount of grassland, water, and unused land, which is not conducive to the improvement of the ecological environment and carbon storage function in the study area. Therefore, the ecological protection scenario is more suitable for protecting the ecological environment and enhancing the carbon storage potential of the Loess Plateau.

By combining the effects of elevation and land use changes on carbon storage under different scenarios, we propose policy recommendations for the optimisation of the future land use structure of the Loess Plateau. (1) Abide by the three red lines of cropland in low-altitude areas (especially areas below 500 m) and guide the rational and scientific planning of construction land and strengthen the protection of high-yield and high-quality cropland on flat and gentle slopes. (2) Continuously promote ecological restoration projects in areas with altitudes over 3000 m as well as gullies and geological fragments. (3) Continue to implement measures to return cropland to forest and grass on slopes, steep slopes, sharp slopes, and poor-quality cropland. These measures increase carbon storage while ensuring food security and cropland quality [29].

4.4. Marginal Contribution, Shortcomings, and Outlook

The PLUS model can not only satisfy the needs of land use change in terms of quantity prediction and spatial allocation but also better explore the causal factors of various types of land use change while accurately simulating complex evolution at the level of multiple types of land use patches. In previous studies, the CLUE-S model was used to predict the land use pattern in the Qi River Basin (located in the Loess Plateau region), and the prediction results yielded an OA of 83.8% and a kappa coefficient of 0.806 [29]. The GeoSOS-FLUS model was used to predict land use patterns at the county level in Changzhou and yielded a kappa coefficient of 0.7743 [19]. In this study, the OA was 87.55% and the kappa coefficient was 0.8224, which indicates that the simulation results of this study are reliable and have high accuracy.

In this study, carbon density was obtained by combining field survey data from the Chinese terrestrial ecosystem carbon density dataset in the study area and parameter correction data with temperature and precipitation. This was a new attempt to determine carbon density compared to previous studies that directly borrowed carbon density data from geographically similar areas. Based on previous studies on carbon density tables of regions with latitudinal and longitudinal positions comparable to that of the Loess Plateau or overlapping with the study area of the Loess Plateau [6,25,26,29,51], we found that the carbon density values of each land use type in this study were within reasonable limits.

Under the influence of human activities, such as urban expansion and restoration, as well as environmental factors, such as temperature, precipitation, and soil, carbon density values change dynamically. Therefore, the carbon density values obtained by using measurement data and model correction will lead to uncertainty in carbon storage estimation results. Therefore, it is necessary for future research to improve the accuracy of ecosystem carbon storage estimations using field monitoring, satellite remote sensing, and other multi-source data acquisition methods. In addition, although a rich system of land use change drivers was constructed in this study, land use change is affected by policies and other factors [29]; therefore, to improve the prediction accuracy of land use types, additional socioeconomic factors and relevant policies can be quantified and incorporated into the driver system in the future [28].

5. Conclusions

This study analyzed land use changes from 2000 to 2020 and used the PLUS model to predict land use patterns for 2035 under different scenarios. A dynamic simulation of the carbon sequestration potential under different development scenarios was conducted based on a quantitative assessment of the spatial and temporal changes in the carbon storage of the ecosystems in the Loess Plateau and the effects of elevation and land use change on carbon storage were quantified. The findings are as follows:

(1) Cropland in the study area decreased significantly from 2000 to 2020, whereas forest, water, and construction land showed an increasing trend. The area of cropland further decreased under the natural growth and ecological protection scenarios, the area of grassland decreased significantly under the cropland protection scenario, and forests and waters were effectively protected under all three scenarios.

(2) From 2000 to 2020, carbon storage increased by 28 Tg, showing an increase of 0.56%, and the carbon density increased by 0.45 t/hm^2, showing an increase of 0.57%. Compared with 2020, by 2035, the carbon storage in the scenarios of natural growth, ecological protection, and cropland protection will increase by 30, 44, and 21 Tg, respectively, and the carbon storage in the three scenarios will be more than 35% in grassland, 30% in forest, and less than 10% in construction land, unused land, and waters.

(3) Carbon storage has obvious spatial heterogeneity, with high carbon density in the northern Qinling Mountains, Taihang Mountains, and Lvliang Mountains and low carbon density in Erdos and its surrounding areas. Regional differences in carbon density are closely related to the spatial distribution of land use types.

(4) The carbon storage in the study area showed an inverted "V" trend of increasing and then decreasing with the increase in elevation, with the peak at about 1500 m. As much as 66% of the carbon storage in the study area is stored at an elevation range of 1000–2000 m. Land use change is the main reason for the increase or decrease in carbon storage under different scenarios. Compared with the other two scenarios, the ecological conservation scenario not only protects the ecological environment but also has a strong carbon storage potential, which may be significant for guiding the formulation of future land use planning on the Loess Plateau.

Author Contributions: Conceptualization, H.Z.; methodology, K.L. and H.Z.; software, K.L.; validation, K.L.; formal analysis, K.L. and H.Z.; investigation, K.L. and H.Z.; resources, H.Z.; data curation, K.L. and C.Z.; writing—original draft preparation, K.L.; writing—review and editing, K.L.; visualization, K.L. and H.X.; supervision, H.Z. and C.Z. project administration, H.Z.; funding acquisition, W.X. and H.X. All authors have read and agreed to the published version of the manuscript.

Funding: This research was funded by the Shaanxi Provincial Department of Education Foundation, NO. 22JK0235, to X.W., the Ankang University Innovation and Entrepreneurship Training Program Project, NO. 202211397015, AKXY2022017, to L.K., and the Ankang University Innovation Team Project, NO. 2022AYSKTD04. Informed Consent Statement to X.H.

Informed Consent Statement: Informed consent was obtained from all subjects involved in the study.

Data Availability Statement: The data presented in this study are available on reasonable request.

Acknowledgments: We thank the beneficial comments from Weiwei Zheng for improving our manuscript.

Conflicts of Interest: The authors declare no conflict of interest.

References

1. Fang, J.Y.; Yu, G.R.; Liu, G.Q.; Zhao, X.Q. Carbon sequestration in Chinese terrestrial ecosystems: Progress of the ecosystem carbon sequestration task force of the strategic pioneer science and technology project of the Chinese Academy of Sciences on "carbon balance certification and related issues in response to climate change. *Bull. Chin. Acad. Sci.* **2015**, *30*, 848–857. [CrossRef]
2. Gao, Y.; He, N.P.; Wang, Y.F. Ecosystem carbon sequestration characteristics and its research progress. *J. Nat. Resour.* **2013**, *28*, 1264–1274.
3. Fang, J.Y.; Kato, T.; Guo, Z.D.; Yang, Y.H.; Hu, H.F.; Shen, H.H.; Zhao, X.; Kishimoto-Mo, A.W.; Tang, Y.H.; Houghton, R.A. Evidence for environmentally enhanced forest growth. *Proc. Natl. Acad. Sci. USA* **2014**, *111*, 9527–9532. [CrossRef]
4. Hu, H.; Zhang, J.H.; Xiong, J.; Zhou, J.; Sun, J.K. Calculation of carbon source and carbon emission reduction pressure analysis in Hebei Province. *Geogr. Geo-Inf. Sci.* **2016**, *32*, 61–67.
5. Tian, D.S.; Fu, B.T.; Lv, Y.P.; Yang, K.; Che, Y. Study on the effect of regional land use change on soil organic carbon storage based on SD and CLUE–S models. *Resour. Environ. Yangtze Basin* **2016**, *25*, 613–620.
6. Qin, M.; Zhao, J.; Feng, C.; Huang, Z.H.; Wen, Y.Y.; Zhang, W.J. Response of carbon storage services to land use change in the Shiyang River Basin ecosystem, 1980–2030. *Acta Ecol. Sin.* **2022**, *23*, 1–12. [CrossRef]
7. Mustafa, A.; Heppenstall, A.; Omrani, H.; Saadi, I.; Cools, M.; Teller, J. Modelling built-up expansion and densification with multinomial logistic regression, cellular automata and genetic algorithm. *Comput. Environ. Urban.* **2018**, *67*, 147–156. [CrossRef]
8. Shen, Q.P.; Chen, Q.; Tang, B.S.; Yeung, S.; Hu, Y.C.; Cheung, G. A system dynamics model for the sustainable land use planning and development. *Habitat Int.* **2009**, *33*, 15–25.
9. Lin, J.J.; Gau, C.C. A TOD planning model to review the regulation of allowable development densities around subway stations. *Land Use Policy* **2006**, *23*, 353–360. [CrossRef]

10. Yang, X.; Zheng, X.Q.; Lv, L.N. A spatiotemporal model of land use change based on ant colony optimization, Markov chain and cellular automata. *Ecol. Model.* **2012**, *233*, 11–19. [CrossRef]
11. Halmy, M.W.A.; Gessler, P.E.; Hicke, J.A.; Salem, B.B. Land use/land cover change detection and prediction in the north–western coastal desert of Egypt using Markov–CA. *Appl. Geogr.* **2015**, *63*, 101–112. [CrossRef]
12. Xu, Q.L.; Wang, Q.; Liu, J.; Liang, H. Simulation of land–use changes using the partitioned ANN–CA model and considering the influence of land–use change frequency. *ISPRS. Int. J. Geo-Inf.* **2021**, *10*, 346. [CrossRef]
13. Guan, D.J.; Zhao, Z.L.; Tan, J. Dynamic simulation of land use change based on Logistic–CA–Markov and WLC–CA–Markov models: A case study in three gorges reservoir area of Chongqing, China. *Environ. Sci. Pollut. Res.* **2019**, *26*, 20669–20688. [CrossRef] [PubMed]
14. Huang, D.Q.; Huang, J.; Liu, T. Delimiting urban growth boundaries using the CLUE–S model with village administrative boundaries. *Land Use Policy* **2019**, *82*, 422–435. [CrossRef]
15. Mamanis, G.; Vrahnakis, M.; Chouvardas, D.; Nasiakou, S.; Kleftoyanni, V. Land use demands for the CLUE–S spatiotemporal model in an agroforestry perspective. *Land* **2021**, *10*, 1097. [CrossRef]
16. Mei, Z.X.; Wu, H.; Li, S.Y. Simulating land–use changes by incorporating spatial autocorrelation and self–organization in CLUE–S modeling: A case study in Zengcheng District, Guangzhou, China. *Front. Earth Sci.* **2018**, *12*, 299–310. [CrossRef]
17. Liang, X.; Liu, X.P.; Li, X.; Chen, Y.M.; Tian, H.; Yao, Y. Delineating multi–scenario urban growth boundaries with a CA–based FLUS model and morphological method. *Landscape Urban Plan.* **2018**, *177*, 47–63. [CrossRef]
18. Xie, Y.; Kuang, H.H.; Wu, J.J.; Cheng, Y.S. Simulation of land use change dynamics in Yubei District, Chongqing City based on CLUE–S model. *Resour. Environ. Yangtze Basin* **2016**, *25*, 1729–1737.
19. Cao, S.; Jin, X.B.; Yang, X.H.; Sun, R.; Liu, J.; Han, B.; Xu, W.Y.; Zhou, Y.K. Compound optimization of county–level land use structure and layout with coupled MOP and GeoSOS–FLUS models. *J. Nat. Resour.* **2019**, *34*, 1171–1185. [CrossRef]
20. Liang, X.; Guan, Q.F.; Clarke, K.C.; Liu, S.S.; Wang, B.Y.; Yao, Y. Understanding the drivers of sustainable land expansion using a patch–generating land use simulation (PLUS) model: A case study in Wuhan, China. *Comput. Environ. Urban.* **2021**, *85*, 101569. [CrossRef]
21. Ma, X.P.; Li, J.; Yu, Y.Y.; Deng, C.H. Spatial service coverage of carbon neutrality in the Qinling Mountains and its simulation prediction. *Acta Ecol. Sin.* **2022**, *42*, 9431–9441. [CrossRef]
22. Zhang, K.; Huang, C.H.; Wang, Z.Y.; Wu, J.Y.; Zeng, Z.Q.; Mu, J.J.; Yang, W.Y. Optimization of the spatial pattern of three lives based on the DTTD–MCR–PLUS model: Taking Changsha city as an example. *Acta Ecol. Sin.* **2022**, *42*, 9957–9970. [CrossRef]
23. Jiang, X.F.; Duan, H.C.; Liao, J.; Song, X.; Xue, X. Land use study of Gan Linggao area in the middle reaches of the Black River Basin based on PLUS–SD coupled model. *Arid Zone Res.* **2022**, *39*, 1246–1258. [CrossRef]
24. Zhang, C.H.; Ju, W.M.; Chen, J.M.; Wang, X.Q.; Yang, L.; Zheng, G. Disturbance-induced reduction of biomass carbon sinks of China's forests in recent years. *Environ. Res. Lett.* **2015**, *10*, 114021. [CrossRef]
25. Liu, Y.; Zhang, J.; Zhou, D.M.; Ma, J.; Dang, R.; Ma, J.J.; Zhu, X.Y. Spatial and temporal variation of carbon storage in Shule River Basin based on InVEST model. *Acta Ecol. Sin.* **2021**, *41*, 4052–4065. [CrossRef]
26. Liu, G.; Li, G.Q.; Li, J.; Zhang, Y.R.; Lu, Q.; Du, S. A study of carbon storage changes and spatial patterns in the Mahta watershed from 1999–2016 based on the InVEST model. *Arid Zone Res.* **2021**, *38*, 267–274. [CrossRef]
27. Mendoza-Ponce, A.; Corona-Núñez, R.; Kraxner, F.; Leduc, S. Identifying effects of land use cover changes and climate change on terrestrial ecosystems and carbon storage in Mexico. *Glob. Environ. Chang.* **2018**, *53*, 12–23. [CrossRef]
28. Zhang, P.P.; Li, Y.H.; Yin, H.R.; Chen, Q.T.; Dong, Q.D.; Zhu, L.Q. Simulation of spatial and temporal changes and dynamics of carbon storage in north-south transition zone ecosystems in China. *J. Nat. Resour.* **2022**, *37*, 1183–1197. [CrossRef]
29. Zhu, W.B.; Zhang, J.J.; Cui, Y.P.; Zheng, H.; Zhu, L.Q. Ecosystem carbon storage assessment based on land use change scenarios: An example from the Qi River Basin in Taihang Mountains. *Acta Geogr. Sin.* **2019**, *74*, 446–459.
30. Liu, G.B.; Shangguan, Z.P.; Yao, W.Y.; Yang, Q.K.; Zhao, M.J.; Dang, X.H.; Guo, M.H.; Wang, G.L.; Wang, B. Ecological effectiveness of the Loess Plateau Ecological Project. *Bull. Chin. Acad. Sci.* **2017**, *32*, 11–19. [CrossRef]
31. Wang, K.B.; Deng, L.; Ren, Z.P.; Shi, W.Y.; Chen, Y.P. Dynamics of ecosystem carbon storage during vegetation restoration on the Loess Plateau of China. *J. Arid. Land.* **2016**, *8*, 207–220. [CrossRef]
32. Cheng, J.M.; Cheng, J.; Yang, X.M.; Liu, W.; Chen, F.R. Spatial distribution characteristics of carbon density in grassland vegetation on the Loess Plateau. *Acta Ecol. Sin.* **2012**, *32*, 226–237. [CrossRef]
33. Gao, Y.; Ma, H.; Cheng, J.M.; An, Y.; Liu, W.; Chen, A. Carbon density of grassland ecosystems in semi–arid areas of the Loess Plateau at different years of closure. *Acta Agrestia Sin.* **2016**, *24*, 28–34.
34. Wang, Y.Y.; Deng, L.; Wu, G.L.; Wang, K.B.; Shangguan, Z.P. Estimates of carbon storage in grassland ecosystems on the Loess Plateau. *Catena* **2018**, *164*, 23–31. [CrossRef]
35. Yang, X.M.; Cheng, J.P.; Meng, L.; Han, J.J. Study on carbon storage and carbon density of Ziwu Ridge forest on Loess Plateau. *J. Soil Water Conserv.* **2010**, *24*, 123–126, 131.
36. Yang, X.M.; Cheng, J.M.; Meng, L. Carbon storage and carbon density characteristics of natural firewood pine forests on the Loess Plateau. *Sci. Soil Water Conserv.* **2010**, *8*, 41–45, 58. [CrossRef]
37. Xue, Z.J.; Ma, L.S.; An, S.S.; Wang, W.Z. Soil organic carbon density and storage at small watershed scale in loess hilly areas. *Acta Ecol. Sin.* **2015**, *35*, 2917–2925. [CrossRef]

38. Zhang, K.; Lv, Y.H.; Fu, B.J.; Yin, L.C.; Yu, D.D. Impacts of vegetation cover changes on ecosystem services and their thresholds in the Loess Plateau. *Acta Geogr. Sin.* **2020**, *75*, 949–960.
39. Li, M.Y.; Shangguan, Z.P.; Deng, L. Spatial Distribution of Ecosystem carbon storage in the Loess Plateau Region and its Influencing Factors. *Acta Ecol. Sin.* **2021**, *41*, 6786–6799.
40. Luo, S.Q.; Hu, X.M.; Sun, Y.; Yan, C.; Zhang, X. Multi–scenario land use change and its impact on carbon storage with coupled PLUS–InVEST model. *Chin. J. Eco-Agric.* **2023**, *31*, 300–314.
41. Xu, L.; He, N.P.; Yu, R.G. 2010s Chinese terrestrial ecosystem carbon density dataset. *China Sci. Data* **2019**, *4*, 90–96. [CrossRef]
42. Li, K.R.; Wang, S.Q.; Cao, M.K. Vegetation and soil carbon storage in China. *Sci. Sin. (Terrae)* **2003**, *33*, 72–80. [CrossRef]
43. Huang, M.; Ji, J.J.; Cao, M.K.; Li, K.R. Simulation of above and below–ground biomass of regional vegetation in China. *Acta Ecol. Sin.* **2006**, *26*, 4156–4163.
44. Piao, S.L.; Fang, J.Y.; He, J.S.; Xiao, Y. Grassland vegetation biomass and its spatial distribution pattern in China. *Chin. J. Plant Ecol.* **2004**, *4*, 491–498.
45. Fang, J.Y.; Liu, G.H.; Xu, S.L. Biomass and net production of forest vegetation in China. *Acta Ecol. Sin.* **1996**, *16*, 497–508.
46. Tui, X.W.; Huang, X.J.; Zheng, Z.Q.; Zhang, M.; Liao, Q.L.; Lai, L.; Lu, J.Y. Impact of land use change on carbon storage in terrestrial ecosystems in Jiangsu Province. *Resour. Sci.* **2011**, *33*, 1932–1939.
47. Chen, G.S.; Yang, Y.S.; Xie, J.S.; Du, Z.X.; Zhang, J. Subsurface carbon allocation in Chinese forests. *Acta Ecol. Sin.* **2007**, *27*, 5148–5157.
48. Alam, S.A.; Starr, M.; Clark, B.J.F. Tree biomass and soil organic carbon densities across the Sudanese woodland savannah: A regional carbon sequestration study. *J. Arid Environ.* **2013**, *89*, 67–76. [CrossRef]
49. An, B.; Xiao, W.W.; Zhang, S.L.; Zhang, J.D. Spatial and temporal characteristics of precipitation days and intensity at different levels on the Loess Plateau from 1960–2017. *Arid Zone Res.* **2021**, *38*, 714–723. [CrossRef]
50. An, B.; Xiao, W.W.; Zhang, S.L.; Zhu, N.; Zhang, J.D. Spatial and temporal variation characteristics of surface temperature on the Loess Plateau from 1960–2017. *Arid Land Geogr.* **2021**, *44*, 778–785.
51. Zhang, Y.; Shi, X.Y.; Tang, Q. Assessment of carbon storage in the upper Fen River region under different land use scenarios. *Acta Ecol. Sin.* **2021**, *41*, 360–373. [CrossRef]